arXiv:1407.5629v1 [hep-th] 21 Jul 2014

21st July 2014

Entanglement entropy of Wilson loops: Holography and matrix models

Simon A. Gentle and Michael Gutperle

Department of Physics and Astronomy
University of California, Los Angeles, CA 90095, USA

sgentle@physics.ucla.edu, gutperle@physics.ucla.edu

Abstract

A half-BPS circular Wilson loop in $\mathcal{N} = 4$ $SU(N)$ supersymmetric Yang-Mills theory in an arbitrary representation is described by a Gaussian matrix model with a particular insertion. The additional entanglement entropy of a spherical region in the presence of such a loop was recently computed by Lewkowycz and Maldacena using exact matrix model results. In this note we utilize the supergravity solutions that are dual to such Wilson loops in a representation with order N^2 boxes to calculate this entropy holographically. Employing the matrix model results of Gomis, Matsuura, Okuda and Trancanelli we express this holographic entanglement entropy in a form that can be compared with the calculation of Lewkowycz and Maldacena. We find complete agreement between the matrix model and holographic calculations.

1 Introduction

In this note we investigate the additional entanglement entropy of a spherical region in $\mathcal{N} = 4$ supersymmetric Yang-Mills theory in the presence of an insertion of a half-BPS circular Wilson loop in a general representation of $SU(N)$ from two distinct points of view: from a matrix model and from gauge/gravity duality.

The expectation value of such a loop in the fundamental representation of $SU(N)$ was first computed in [1, 2]. A special conformal transformation maps the circle to a straight line, whilst sending one point to infinity. It is known that the expectation value for the line is exactly unity and so the non-trivial value for the circular loop must come from the point at infinity. This was confirmed in [3], wherein it was shown using localization techniques that the circular loop is described by a Gaussian matrix model for arbitrary representations of $SU(N)$.

In [4], Lewkowycz and Maldacena related this entanglement entropy to the expectation value of a circular loop and of the stress tensor in the presence of this loop by mapping the problem into the calculation of thermal entropy for a finite temperature field theory on a hyperbolic space [5]. Since both quantities can be calculated through localization by a matrix model, it is possible to obtain an expression for the entanglement entropy in the large N, large λ limit in an arbitrary representation.

The holographic description of Wilson loops in Type IIB string theory goes back to [6, 7] wherein it was shown that the Wilson loop in the fundamental representation is described by a fundamental string in $AdS_5 \times S^5$. For larger representations the fundamental string gets replaced by a probe D-brane. It was shown in [8, 9, 10] that a Wilson loop in the k-th symmetric (or antisymmetric) representation is described by a D3 (or D5) brane with k units of electric flux on its world volume.

A general representation is characterized by a Young tableau. If the number of boxes becomes of order N^2 then the probe-brane description breaks down and is replaced by a fully back-reacted "bubbling" solution. Such solutions were first constructed in [11], building on the earlier work of [12, 13, 14, 15]. Our first goal in this note is to calculate the entanglement entropy in the presence of a half-BPS circular Wilson loop by applying the Ryu-Takayanagi prescription [16, 17] to these static Type IIB supergravity solutions.

This holographic entanglement entropy can then be expressed in a form that makes comparison with the matrix model calculation possible. We show that in the saddle-point approximation of the matrix model, and at large λ, the two calculations agree. In our opinion this agreement is non-trivial since the two ways to calculate the entanglement entropy look very different from the outset. One can interpret this agreement as a non-trivial check of

the calculation of [4], or alternatively as further confirmation of the map proposed in [18] between the supergravity solutions and the matrix model description of the circular Wilson loop.

Before moving forward, let us clarify the geometry of our setup. We are always interested in the circular Wilson loop. The entanglement entropy of the half-space that is intersected once by a circular loop is conformally equivalent to a straight line threading a spherical region with the point at infinity included. We will find it more convenient to work with the latter setup when we compute the entanglement entropy holographically.

This note is organized as follows. In section 2 we review the matrix model description of our Wilson loop and state the formula given by Lewkowycz and Maldacena for the entanglement entropy. In section 3 we review the supergravity solutions dual to half-BPS Wilson loops constructed in [11] and their relation to the matrix model data. In section 4 we calculate the entanglement entropy holographically and express it in a form that can be compared with the matrix model results. Careful attention is paid to the regularization of the resulting integrals. In section 5 the matrix model and holographic calculations are compared and it is shown that if the matrix model saddle-point equations are satisfied then the two expressions agree. We close with a brief discussion of our results in 6. Some calculational details regarding the regularization and holographic map of cut-offs are given in appendix A. The proof of the equivalence between the matrix model and holographic entanglement entropy is provided in appendix B.

2 Half-BPS Wilson loops and matrix models

The expectation value of a half-BPS circular Wilson loop in $\mathcal{N}=4$ $SU(N)$ supersymmetric Yang-Mills theory is described by a Gaussian matrix model. This exact result was demonstrated in [3] using localization techniques. In particular,

$$\langle W_{\mathcal{R}} \rangle = \frac{1}{\mathcal{Z}} \int [dM] \, \mathrm{tr}_{\mathcal{R}} \, e^{M'} \exp\left(-\frac{2N}{\lambda} \mathrm{tr} \, M^2 \right) \tag{2.1}$$

where M is an $N \times N$ Hermitian matrix, $M' \equiv M - \frac{1}{N}(\mathrm{tr}\, M)\mathbb{1}_{N\times N}$ is its trace-removed form and $\mathcal{R}$ is the representation of $SU(N)$. In this note we focus on large representations for which the number of boxes in each row or column of the corresponding Young tableau is of order N.

One can evaluate $\langle W_{\mathcal{R}} \rangle$ using saddle-point methods. To leading order in the saddle-point approximation, i.e. at large N with λ held fixed, the normalized expectation value of the Wilson loop satisfies

$$\log \langle W_{\mathcal{R}} \rangle = -\left(\mathcal{S}_{\mathrm{mat}} - \mathcal{S}_0 \right) \tag{2.2}$$

where $\mathcal{S}_{\rm mat}$ and $\mathcal{S}_0$ denote the on-shell effective action of the Gaussian matrix model with and without the insertion of the Wilson loop, respectively. At large λ it was shown in [18] that the effective action can be written as follows:

$$-\mathcal{S}_{\rm mat} = N\sum_{I=1}^{g+1}\int_{\mathcal{C}_I} dx\,\rho(x)\left(-\frac{2N}{\lambda}\,x^2+\hat{K}_I\,x\right)+N^2\int_{\mathcal{C}\times\mathcal{C}} dx\,dy\,\rho(x)\,\rho(y)\log|x-y| \tag{2.3}$$

Let us define the terms in this equation. The matrix M is decomposed into $g+1$ blocks of size $n_I\times n_I$. For large N, the eigenvalues of M form a continuous distribution $\rho(x)$ over $g+1$ intervals $\mathcal{C}_I$. The $I^{\rm th}$ interval contains a fraction n_I/N of the eigenvalues and $\mathcal{C}$ is the union of these intervals. The interactions between the eigenvalues on the intervals simplify at large λ to the logarithmic repulsion term shown. The Young tableau of interest consists of g blocks and the $I^{\rm th}$ block has n_I rows of length K_I. We define $\hat{K}_I\equiv K_I-|\mathcal{R}|/N$, where $|\mathcal{R}|$ is the total number of boxes.[1] We also note that $K_{g+1}=0$ and the following relations:

$$\frac{n_I}{N}=\int_{\mathcal{C}_I} dx\,\rho(x)\quad\text{and}\quad\sum_I\int_{\mathcal{C}_I} dx\,\rho(x)=\int_{\mathcal{C}} dx\,\rho(x)=1 \tag{2.4}$$

The eigenvalue distribution $\rho(x)$ satisfies the continuum version of the saddle-point equation:

$$-4x+\frac{\lambda}{N}\,\hat{K}_I+2\mathrm{P}\int_{\mathcal{C}} dy\,\frac{\rho(y)}{x-y}=0\quad\text{for}\quad x\in\mathcal{C}_I \tag{2.5}$$

This is a set of singular integral equations that can be solved by introducing the resolvent $\omega(z)$, which takes the following form in the large N limit:

$$\omega(z)=\lambda\int_{\mathcal{C}} dx\,\frac{\rho(x)}{z-x} \tag{2.6}$$

As a function of the spectral parameter z, this is analytic on the whole complex plane except on the intervals $\mathcal{C}_I$, where it has a discontinuity as one crosses each interval. We can re-write (2.5) in terms of these discontinuities as

$$-4x+\frac{\lambda}{N}\,\hat{K}_I+\omega_+(x)+\omega_-(x)=0\quad\text{for}\quad x\in\mathcal{C}_I \tag{2.7}$$

where $\omega_\pm(x)\equiv\omega(x\pm i\epsilon)$.

The action in the absence of the loop is given by (2.3) for a single interval (i.e. $g=0$), in which case the eigenvalues are distributed according to the Wigner semicircle rule:

$$\mathcal{S}_0=N^2\left(-\log\sqrt{\lambda}+\log 2+3/4\right) \tag{2.8}$$

$$\rho_{(0)}(x)=\frac{2}{\pi\lambda}\sqrt{\lambda-x^2}\quad\text{for}\quad x\in\left[-\sqrt{\lambda},\sqrt{\lambda}\right] \tag{2.9}$$

[1] The parameters K_I and $\hat{K}_I$ are associated with $U(N)$ and $SU(N)$ gauge groups, respectively [18].

A useful result for a single interval that we shall need later on is

$$\int_{\mathcal{C}\times\mathcal{C}} dx\, dy\, \rho(x)\, \rho(y) \log|x-y| = \log\sqrt{\lambda} - \log 2 - \frac{1}{4} \tag{2.10}$$

Next we review the calculation of Lewkowycz and Maldacena [4]. The quantity of interest is the entanglement entropy relative to the vacuum of a spherical region of radius R threaded by a half-BPS circular Wilson loop. They showed that this can be expressed as a sum of the expectation value of this loop and the one-point function of the stress tensor in the presence of this loop. The latter is fixed by conformal symmetry up to an overall coefficient h_W known as the scaling weight of the Wilson loop. Their formula is

$$\Delta S_{\mathcal{A}} = \log\langle W_{\mathcal{R}}\rangle + 8\pi^2 h_W \tag{2.11}$$

using the sign convention of [19]. It was shown in [19] that the scaling weight is related to the difference between the second moment of the matrix model eigenvalue distribution with the Wilson loop and without, $\Delta\rho_2 \equiv \rho_2 - \rho_2^{(0)}$, via

$$h_W = -\frac{N^2}{3\pi^2\lambda}\,\Delta\rho_2 \tag{2.12}$$

where

$$\rho_2 \equiv \int_{\mathcal{C}} dx\, \rho(x)\, x^2 \quad \text{and} \quad \rho_2^{(0)} = \frac{\lambda}{4} \tag{2.13}$$

In section 5 we will show that our holographic computation of the entanglement entropy agrees precisely with (2.11).

3 Supergravity description of half-BPS Wilson loops

In this section we review the features of the supergravity solutions that are important for the present work. Their derivation and more details can be found in [11]. These static solutions have isometry group $SO(2,1)\times SO(3)\times SO(5)$ and preserve 16 out of the total 32 supersymmetries, which are the same symmetries as a half-BPS circular Wilson loop. The ten-dimensional metric takes the form of a Janus-like ansatz [20] using a fibration of $AdS_2\times S^2\times S^4$ over a two-dimensional Riemann surface Σ with boundary $\partial\Sigma$. The metric can be written in the form[2]

$$ds^2 = f_1^2\, ds^2_{AdS_2} + f_2^2\, ds^2_{S^2} + f_4^2\, ds^2_{S^4} + 4\sigma^2 d\Sigma^2, \quad d\Sigma^2 = |dw|^2 \tag{3.1}$$

[2]We deviate slightly from the notation in [11] and call a metric function σ instead of ρ to prevent confusion between the metric functions and the matrix model eigenvalue distribution.

where $ds^2_{S^2}$ and $ds^2_{S^4}$ are the metrics on the unit radius two and four sphere, respectively. The metric on the unit radius Euclidean AdS_2 in Poincaré half-plane coordinates is given by

$$ds^2_{AdS_2} = \frac{dv^2 + d\tau^2}{v^2} \tag{3.2}$$

These half-BPS solutions are characterized by two harmonic functions h_1, h_2 defined on Σ. The metric functions are most easily expressed in terms of the following auxiliary quantities:

$$\begin{aligned} W &= \partial_w h_1 \partial_{\bar{w}} h_2 + \partial_w h_2 \partial_{\bar{w}} h_1, \qquad & V &= \partial_w h_1 \partial_{\bar{w}} h_2 - \partial_w h_2 \partial_{\bar{w}} h_1 \\ N_1 &= 2h_1 h_2\, \partial_w h_1 \partial_{\bar{w}} h_1 - h_1^2 W, \qquad & N_2 &= 2h_1 h_2\, \partial_w h_2 \partial_{\bar{w}} h_2 - h_2^2 W \end{aligned} \tag{3.3}$$

The expressions for the dilaton Φ and the metric functions are then given by

$$\begin{gathered} e^{2\Phi} = -\frac{N_2}{N_1}, \qquad \sigma^8 = -\frac{W^2 N_1 N_2}{h_1^4 h_2^4} \\ f_1^4 = -4e^{\Phi} h_1^4 \frac{W}{N_1}, \qquad f_2^4 = 4e^{-\Phi} h_2^4 \frac{W}{N_2}, \qquad f_4^4 = 4e^{-\Phi} \frac{N_2}{W} \end{gathered} \tag{3.4}$$

For the regular solutions constructed in [11] the Riemann surface Σ is taken to be the lower half-plane $w \in \mathbb{C}$, $\operatorname{Im} w < 0$. The $AdS_5 \times S^5$ vacuum (i.e. no Wilson loop is present) is realized as follows:

$$h_1 \sim \sqrt{1 - w^2} + \sqrt{1 - \bar{w}^2}, \qquad h_2 \sim i(w - \bar{w}) \tag{3.5}$$

Note that in this case the harmonic function h_1 satisfies the following boundary conditions on the real line, which is the boundary of Σ: Neumann boundary conditions inside the interval $\operatorname{Re} w \in [-1, 1]$ and vanishing Dirichlet boundary conditions outside this interval.

The general regular solutions are constructed by modifying the boundary conditions for the harmonic function h_1. A genus g solution is characterized by $2g + 2$ real numbers

$$e_i \in \mathbb{R}, \quad i = 1, 2, \ldots, 2g; \quad e_0 = +\infty, \quad e_{2g+1} = -\infty \tag{3.6}$$

with the ordering $e_i > e_{i+1}$. The boundary conditions for h_1 alternate as follows:

$$h_1|_{\operatorname{Im} w = 0} : \begin{cases} \text{Neumann}, & \operatorname{Re} w \in [e_{2i}, e_{2i-1}] \\ \text{Dirichlet}, & \operatorname{Re} w \in [e_{2i-1}, e_{2i-2}] \end{cases} \tag{3.7}$$

For example, the explicit $g = 1$ solution can be expressed in terms of elliptic integrals. Full details of this solution, including formulae for the antisymmetric tensor fields, can be found in [11, 18, 21] but will not be needed in this paper. It was shown in [18] that there is an exact identification between the data for the supergravity solution encoded in the boundary conditions (3.7) and the representation $\mathcal{R}$ of the circular Wilson loop — see figure 1.

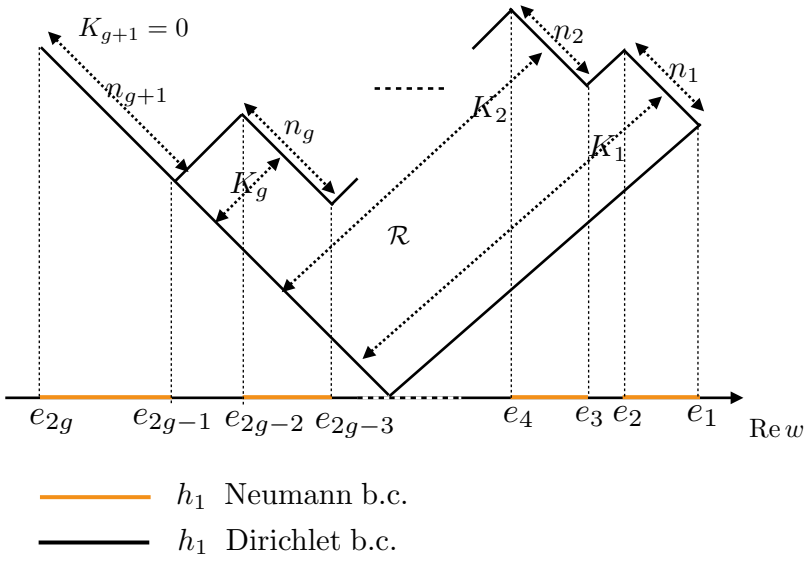

Figure 1: The map between the supergravity data specified in (3.7) and the data of the representation $\mathcal{R}$ of the circular Wilson loop specified by $\{n_I, K_I\}$. The figure is adapted from [18].

A map between the supergravity solutions and the matrix model quantities was also found in [18]. The harmonic functions are given in terms of the spectral parameter z and matrix model resolvent $\omega(z)$ via

$$h_1 = \frac{i\alpha'}{8g_s}\left[2(z-\bar{z}) - (\omega - \bar{\omega})\right] \quad \text{and} \quad h_2 = \frac{i\alpha'}{4}(z-\bar{z}) \tag{3.8}$$

Here we identify the spectral parameter z with the coordinate we use on Σ: $z \equiv w$. It takes values in the lower half-plane. In the following sections we will exploit this map to show that the holographic and matrix model calculations give the same results for the entanglement entropy of our Wilson loop.

4 Holographic calculation of entanglement entropy

The Ryu-Takayanagi prescription [16, 17] states that the entanglement entropy of a spatial region $\mathcal{A}$ is given by the area of a co-dimension two minimal surface $\mathcal{M}$ in the bulk that is anchored on the AdS boundary at $\partial\mathcal{A}$:

$$S_{\mathcal{A}} = \frac{A_{\min}}{4G_N^{(10)}} \tag{4.1}$$

Since we are dealing with static states of our CFT, this surface lies on a constant time slice. If this surface is not unique, we choose the one whose area is minimal among all such surfaces

homologous to $\mathcal{A}$.[3]

The spacetime of interest is an $AdS_2 \times S^2 \times S^4$ fibration over Σ. We consider a surface $\mathcal{M}$ parametrized by integrating over the S^2, S^4 and Σ and choosing the spatial AdS_2 coordinate in (3.2) to depend on Σ, i.e. $v = v(z, \bar{z})$. The area functional becomes

$$A(\mathcal{M}) = 2\,\mathrm{Vol}(S^2)\,\mathrm{Vol}(S^4) \int d^2z\, f_2^2\, f_4^4\, \sigma^2 \sqrt{1 + \frac{f_1^2}{v^2\sigma^2} \frac{\partial v}{\partial z} \frac{\partial v}{\partial \bar{z}}} \tag{4.2}$$

Following [23, 24] it is easy to see that the minimal area surface is given by setting $v(z, \bar{z})$ to a constant, since the second term under the square root in (4.2) is always positive and vanishes only for constant v. We will show in appendix A that the choice $v = R$ in this AdS_2 slicing corresponds at the boundary to our desired region $\mathcal{A}$: a sphere of radius R in Poincaré slicing.

The minimal area is therefore

$$\begin{aligned} A_{\min} &= 2\,\mathrm{Vol}(S^2)\,\mathrm{Vol}(S^4) \int d^2z\, f_2^2\, f_4^4\, \sigma^2 \\ &= -\frac{2^9\pi^3}{3} \int d^2z\, \left\{ 2h_2^2\, \partial_z h_1 \partial_{\bar{z}} h_1 - h_1 h_2\, (\partial_z h_1 \partial_{\bar{z}} h_2 + \partial_{\bar{z}} h_1 \partial_z h_2) \right\} \end{aligned} \tag{4.3}$$

where we used (3.3) and (3.4) to express $A_{\min}$ in terms of the harmonic functions $h_{1,2}$.

For the $g = 1$ solution the entanglement entropy can in principle be evaluated by substituting the explicit expressions given in [11] for the harmonic functions and performing the integrals. Since our goal is to compare the holographic entanglement entropy to the matrix model calculation for arbitrary g, we instead use (3.8) to rewrite the area of the minimal surface in terms of the matrix model resolvent $\omega(z)$:

$$\begin{aligned} A_{\min} = -\frac{\pi^3 \alpha'^4}{6 g_s^2} \int d^2z\, \big\{ & 2(z-\bar{z})^2 (\partial_z \omega + \partial_{\bar{z}} \bar{\omega}) - 4(z-\bar{z})(\omega - \bar{\omega}) \\ & -2(z-\bar{z})^2 \partial_z \omega\, \partial_{\bar{z}} \bar{\omega} + (z-\bar{z})(\omega - \bar{\omega})(\partial_z \omega + \partial_{\bar{z}} \bar{\omega}) \big\} \end{aligned} \tag{4.4}$$

Note that we have dropped the $\partial_z \bar{\omega}$ and $\partial_{\bar{z}} \omega$ terms from (4.4): these are proportional to delta functions $\delta(z - x, \bar{z} - x)$, which integrate to zero against the $(z - \bar{z})$ factors because x in (2.6) is real.

We rewrite the expression for $A_{\min}$ by inserting the spectral representation (2.6) and performing the integration over z after exchanging the order of integration. Since the integrals are divergent one has to take care with the regularization. The details of this calculation are presented in appendix A and the final result for the holographic entanglement entropy is

$$S_{\mathcal{A}} = N^2 \left[\frac{R^2}{\varepsilon^2} - \log \frac{R}{\varepsilon} - \log \sqrt{\lambda} + \frac{3}{4} - \frac{2\rho_2}{3\lambda} + \int_{\mathcal{C}\times\mathcal{C}} dx\, dy\, \rho(x)\, \rho(y) \log |x - y| \right] \tag{4.5}$$

[3] This minimal surface prescription was recently established on a firm footing by the analysis of [22].

where R is the radius of the spherical entangling region and ε is the UV cut-off defined in the Fefferman-Graham chart near the AdS boundary.

This is the result for a general number of intervals, describing a Wilson loop in a general representation $\mathcal{R}$. The same expression for a single interval gives the area of the minimal surface in $AdS_5 \times S^5$. Thus, the result for the entanglement entropy of the vacuum is

$$S_{\mathcal{A}}^{(0)} = N^2 \left[\frac{R^2}{\varepsilon^2} - \log \frac{2R}{\varepsilon} + \frac{1}{3} \right] \tag{4.6}$$

where we used (2.10) and $\rho_2^{(0)} = \lambda/4$. The logarithmic term is universal and has coefficient N^2 as required.

The additional entanglement entropy due to the Wilson loop is found by subtracting the above two results:

$$\Delta S_{\mathcal{A}} = N^2 \left[\int_{\mathcal{C}\times\mathcal{C}} dx\, dy\, \rho(x)\, \rho(y) \log|x-y| - \frac{2\Delta\rho_2}{3\lambda} - \left(\log\sqrt{\lambda} - \log 2 - \frac{1}{4} \right) \right] \tag{4.7}$$

5 Comparison

Now we are ready to compare the holographic calculation with the matrix model result (2.11). Using (2.2), (2.3) and (2.8) we can write

$$\begin{aligned} \log\langle W_{\mathcal{R}} \rangle = N \sum_{I=1}^{g+1} \int_{\mathcal{C}_I} dx\, \rho(x) \left(-\frac{2N}{\lambda}\, x^2 + \hat{K}_I\, x \right) + N^2 \int_{\mathcal{C}\times\mathcal{C}} dx\, dy\, \rho(x)\, \rho(y) \log|x-y| \\ + N^2 \left(-\log\sqrt{\lambda} + \log 2 + \frac{3}{4} \right) \end{aligned} \tag{5.1}$$

Adding this to the expression for the scaling weight h_W in (2.12) we find that our result for $\Delta S_{\mathcal{A}}$ in (4.7) appears, along with two additional terms:

$$\log\langle W_{\mathcal{R}} \rangle + 8\pi^2 h_W = \Delta S_{\mathcal{A}} - \frac{4N^2}{\lambda}\, \Delta\rho_2 + N \sum_I \int_{C_I} dx\, \rho(x)\, \hat{K}_I\, x \tag{5.2}$$

In appendix B we show that the last two terms on the right hand side of (5.2) sum to zero, once we impose the saddle-point equation (2.7). Consequently we find complete agreement between the holographic calculation and the Lewkowycz and Maldacena result.

6 Discussion

In this note we provided a proof of the agreement between two methods to calculate the entanglement entropy in the presence of a half-BPS circular Wilson loop: the replica method of Lewkowycz and Maldacena and the (suitably-modified) holographic prescription of Ryu

and Takayanagi. An essential ingredient in our proof was the matrix model description of the expectation value of this Wilson loop (and related moments) in the saddle-point approximation.

The original prescription for the calculation of holographic entanglement entropy considered the area of minimal surfaces in AdS spaces. Here we generalized this prescription due to the fact that the spacetime is a fibration of $AdS_2 \times S^2 \times S^4$ over a Riemann surface Σ. Specifically, our prescription takes the minimal surface to span the spheres as well as the Riemann surface Σ. Note that the same prescription has been used in related holographic calculations of the boundary entropy of BPS interface solutions [25], which are constructed using similar fibrations [26, 27]. It was shown in [25] that the holographic boundary entropy agreed with the CFT results [28]. In our opinion, the new example of a highly non-trivial agreement found in the present note further strengthens the case that the generalized prescription is correct.

As mentioned in section 1, we could equally well have choosen global coordinates (i.e. the hyperbolic disk) in (3.2) and found the same minimal surface. The UV cut-off is blind to this difference because the coordinate transformation between Poincaré and global AdS_2 does not involve the five-dimensional radial coordinate. Consequently the result for $\Delta S_{\mathcal{A}}$ would not be modified.

Lewkowycz and Maldacena also calculated the entanglement entropy for the Wilson loop insertion in the three-dimensional $\mathcal{N} = 6$ supersymmetric Chern-Simons matter (ABJM) theory in [4]. Unfortunately, we cannot conduct a similar consistency check for this case because the supergravity solutions analogous to the Wilson loop solution of [11] are not known. It would be interesting to see if such solutions can be developed using the methods of [29].

Acknowledgements

It is a pleasure to thank Matthew Headrick, Per Kraus, Aitor Lewkowycz and Mukund Rangamani for useful discussions. SAG would also like to thank the Aspen Center for Physics for hospitality during the concluding stages of this project. This work was supported in part by National Science Foundation grants PHY-13-13986 and PHYS-1066293.

A Integrals and regularization

In this appendix we carefully discuss the regularization and evaluation of the integrals that make up the area of the minimal surface (4.4). For clarity we split the integrals into two terms and evaluate them separately:

$$I_1 \equiv \int d^2z \, \left\{2(z-\bar{z})^2(\partial_z\omega + \partial_{\bar{z}}\bar{\omega}) - 4(z-\bar{z})(\omega-\bar{\omega})\right\} \tag{A.1}$$

$$I_2 \equiv \int d^2z \, \left\{-2(z-\bar{z})^2\partial_z\omega\,\partial_{\bar{z}}\bar{\omega} + (z-\bar{z})(\omega-\bar{\omega})(\partial_z\omega + \partial_{\bar{z}}\bar{\omega})\right\} \tag{A.2}$$

To evaluate these integrals we insert the spectral representation (2.6) for the resolvents ω and perform the integrals over z first.

First consider I_1, which is linear in ρ. Working in the Cartesian coordinates $z = x + i\,y$ we obtain

$$I_1 = -64\,\lambda \int_{\mathcal{C}} dx_1\,\rho(x_1) \int_{-\infty}^{\infty} dx \int_{-\infty}^{0} dy\, \frac{y^4}{((x-x_1)^2+y^2)^2} \tag{A.3}$$

This integral is quadratically divergent at large y. Superficially it appears that one can remove x_1 from I_1 by a shift in the integration variable. However, as is well known from the evaluation of Feynman diagrams, such arguments fail for integrals that have power law divergences.

To see this, we work in polar coordinates $z = \sqrt{\lambda}\,r\,e^{-i\phi}$ instead. The factor of $\sqrt{\lambda}$ will enable a cleaner identification of the Fefferman-Graham cut-off — see the end of this appendix. We obtain

$$I_1 = -64\,\lambda^4 \int_{\mathcal{C}} dx_1\,\rho(x_1) \int_0^{\infty} dr \int_0^{\pi} d\phi\, \frac{r^5 \sin^4\phi}{(r^2\lambda - 2rx_1\sqrt{\lambda}\cos\phi + x_1^2)^2} \tag{A.4}$$

Note that the integral is quadratically divergent at large r. To regularize this divergence we cut off the radial integration at some large r_c. The angular integral can be performed and we find

$$\int_0^{\pi} d\phi\, \frac{r^5\sin^4\phi}{(r^2\lambda - 2rx_1\sqrt{\lambda}\cos\phi + x_1^2)^2} = \begin{cases} \frac{3\pi r}{8\lambda^2}, & r > \frac{|x_1|}{\sqrt{\lambda}} \\ \frac{3\pi r^5}{8x_1^4}, & r < \frac{|x_1|}{\sqrt{\lambda}} \end{cases} \tag{A.5}$$

Performing the regulated integral over r we obtain

$$I_1 = -64\,\lambda^4 \int_{\mathcal{C}} dx_1\,\rho(x_1) \left[\frac{3\pi}{8}\left(\int_{\frac{|x_1|}{\sqrt{\lambda}}}^{r_c} dr\,\frac{r}{\lambda^2} + \int_0^{\frac{|x_1|}{\sqrt{\lambda}}} dr\,\frac{r^5}{x_1^4}\right)\right] = 12\pi\lambda^2\left(\frac{2\rho_2}{3\lambda} - r_c^2\right) \tag{A.6}$$

where we used

$$\int_{\mathcal{C}} dx\,\rho(x) = 1 \quad \text{and} \quad \rho_2 = \int_{\mathcal{C}} dx\,\rho(x)\,x^2 \tag{A.7}$$

Note that in addition to the quadratically divergent piece, proportional to r_c^2, there is also a finite piece.

The integral in (A.2) is quadratic in ρ and can be expressed as

$$I_2 = -\frac{\lambda^2}{2}\int_{\mathcal{C}} dx_1\,\rho(x_1)\int_{\mathcal{C}} dx_2\,\rho(x_2) \\ \times\int d^2z\,(z-\bar{z})^4\,\frac{(x_1-x_2)^2-(z-x_1)(\bar{z}-x_2)-(\bar{z}-x_1)(z-x_2)}{|z-x_1|^4|z-x_2|^4} \tag{A.8}$$

where we have symmetrized appropriately. Note that the integral over z is logarithmically divergent instead of quadratically divergent. It is therefore possible to shift the integration variable as $z = x_1 + \sqrt{\lambda}\,r\,e^{-i\phi}$ such that the integral will only depend on $\Delta x = x_1 - x_2$. After this shift we find

$$I_2 = 16\lambda^3\int_{\mathcal{C}} dx_1\,\rho(x_1)\int_{\mathcal{C}} dx_2\,\rho(x_2) \\ \times\int_0^{r_c} dr\int_0^{\pi} d\phi\,r\,\frac{2r^2\lambda+2r\Delta x\sqrt{\lambda}\cos\phi-\Delta x^2}{(r^2\lambda+2r\Delta x\sqrt{\lambda}\cos\phi+\Delta x^2)^2}\,\sin^4\phi \tag{A.9}$$

Using

$$\int_0^{\pi} d\phi\,r\,\frac{2r^2\lambda+2r\Delta x\sqrt{\lambda}\cos\phi-\Delta x^2}{(r^2\lambda+2r\Delta x\sqrt{\lambda}\cos\phi+\Delta x^2)^2}\,\sin^4\phi = \begin{cases} \frac{3\pi}{4\lambda r}-\frac{7\pi\Delta x^2}{8\lambda^2 r^3}, & r>\frac{|\Delta x|}{\sqrt{\lambda}} \\ \frac{\pi\lambda r^3}{4\Delta x^4}-\frac{3\pi r}{8\Delta x^2}, & r<\frac{|\Delta x|}{\sqrt{\lambda}} \end{cases} \tag{A.10}$$

and dropping terms that tend to zero as $r_c\to\infty$, the regulated integral (A.9) becomes

$$I_2 = 12\pi\lambda^2\left(\log r_c - \frac{3}{4} + \log\sqrt{\lambda} - \int_{\mathcal{C}\times\mathcal{C}} dx_1\,dx_2\,\rho(x_1)\,\rho(x_2)\log|\Delta x|\right) \tag{A.11}$$

Next we substitute the results (A.6) and (A.11) into (4.4) in order to evaluate the holographic entanglement entropy:

$$\begin{aligned} S_{\mathcal{A}} &= \frac{A_{\min}}{4G_N^{(10)}} \\ &= \left(-\frac{\pi^3\alpha'^4}{6g_s^2}\right)\frac{1}{2^5\pi^6\alpha'^4}\,(12\pi)(4\pi g_s N)^2\left[\frac{2\rho_2}{3\lambda} - r_c^2 + \log r_c - \frac{3}{4} + \log\sqrt{\lambda}\right. \\ &\quad \left. - \int_{\mathcal{C}\times\mathcal{C}} dx\,dy\,\rho(x)\,\rho(y)\log|x-y|\right] \\ &= N^2\left[r_c^2 - \log r_c - \log\sqrt{\lambda} + \frac{3}{4} - \frac{2\rho_2}{3\lambda} + \int_{\mathcal{C}\times\mathcal{C}} dx\,dy\,\rho(x)\,\rho(y)\log|x-y|\right] \end{aligned} \tag{A.12}$$

where we used $4G_N^{(10)} = \frac{1}{4\pi}(2\pi)^7\alpha'^4$ and also $\lambda = 4\pi g_s N$ where appropriate.

We still need to show how the radial cut-off r_c is related to the UV cut-off. At large r, any bubbling geometry of the form (3.1) asymptotes to $AdS_5\times S^5$:

$$ds^2 = L^2\left\{\frac{dr^2}{r^2} + r^2\left(ds^2_{AdS_2} + ds^2_{S^2}\right) + d\phi^2 + \sin^2\phi\,ds^2_{S^4}\right\} \tag{A.13}$$

with the AdS_2 metric given in (3.2).[4] Any asymptotically AdS metric may be written as a Fefferman-Graham expansion, at least locally, in the asymptotically AdS region. We write this as a power series in u about $u = 0$, which for us takes the form

$$ds^2 = L^2 \left\{ \frac{1}{u^2} \left(du^2 + d\tau^2 + dy^2 + y^2 ds^2_{S^2} \right) + d\chi^2 + \sin^2 \chi \, ds^2_{S^4} \right\} \tag{A.14}$$

plus subleading corrections. Comparing (A.13) and (A.14), at leading order we identify

$$\frac{u}{v} = \frac{1}{r}, \quad y = v, \quad \chi = \phi \tag{A.15}$$

Therefore, the large-r cut-off is related to the UV cut-off $u = \varepsilon$ on the minimal surface $v = R$ near the boundary via

$$r_c = \frac{R}{\varepsilon} \tag{A.16}$$

Substituting this result into (A.12) we arrive at the final answer (4.5) for the entanglement entropy.

It is straightforward to show how the surface $v = R$ in AdS_2 slicing ends on a sphere of radius R at the boundary in Poincaré slicing. Near the boundary we have the map (A.15) between the two slicings. It is well known (see [16, 17], for example) that the equation for a minimal surface anchored on a boundary sphere of radius R in Poincaré slicing (A.14) is

$$u(y)^2 + y^2 = R^2 \tag{A.17}$$

Close to the boundary, the first term goes to zero and $y \to v$. Thus we find $v = R$, as required.

B Proof of equivalence

In this appendix we give the details of the proof that the matrix model and holographic entanglement entropies are equal. The relation we have to prove is

$$-\frac{4}{\lambda} \Delta\rho_2 + \frac{1}{N} \sum_I \int_{C_I} dx \, \rho(x) \, \hat{K}_I \, x = 0 \tag{B.1}$$

First we substitute for $\Delta\rho_2$ using (2.13) and deduce that the left-hand side of this relation can be written

$$\text{LHS} = 1 + \sum_I \int_{C_I} dx \, \rho(x) \, x \left(-\frac{4}{\lambda} \, x + \frac{1}{N} \, \hat{K}_I \right) \tag{B.2}$$

[4] To see this, substitute $z = \sqrt{\lambda} \, r \, e^{-i\phi}$ and the $g = 0$ resolvent into (3.8) and construct the metric.

Next we impose the saddle-point equations (2.7) and find

$$\text{LHS} = 1 - \int_{-\infty}^{\infty} dx\, \rho(x)\, x\, \frac{\omega_+(x) + \omega_-(x)}{\lambda} \tag{B.3}$$

We are able to extend the integration range to the real line since $\rho(x)$ vanishes outside the intervals $\mathcal{C}_I$. Following the conventions of [18], the eigenvalue density can be expressed in terms of the resolvents $\omega_\pm(x) = \omega(x \pm i\epsilon)$ as

$$\rho(x) = \frac{i}{2\pi\lambda} \left(\omega_+(x) - \omega_-(x)\right) \tag{B.4}$$

and hence (B.3) can be written as

$$\text{LHS} = 1 + \frac{1}{2\pi i}\, \frac{1}{\lambda^2} \int_{-\infty}^{\infty} dx\, x \left(\omega_+^2(x) - \omega_-^2(x)\right) \tag{B.5}$$

Now we employ the integral representation of $\omega(z)$ given in (2.6) to find

$$\begin{aligned}\text{LHS} = 1 + \frac{1}{2\pi i} \int_{-\infty}^{\infty} dx\, x \int_{\mathcal{C}} dx_1 \int_{\mathcal{C}} dx_2 \Bigg(& \frac{\rho(x_1)}{x - x_1 + i\epsilon}\, \frac{\rho(x_2)}{x - x_2 + i\epsilon} \\ & - \frac{\rho(x_1)}{x - x_1 - i\epsilon}\, \frac{\rho(x_2)}{x - x_2 - i\epsilon} \Bigg)\end{aligned} \tag{B.6}$$

First we exchange the order of integration. The relevant integral over x can be performed using the residue theorem and we find

$$\int_{-\infty}^{\infty} dx\, x \left(\frac{1}{x - x_1 + i\epsilon}\, \frac{1}{x - x_2 + i\epsilon} - \frac{1}{x - x_1 - i\epsilon}\, \frac{1}{x - x_2 - i\epsilon} \right) = -2\pi i \tag{B.7}$$

Then we are simply left with

$$\text{LHS} = 1 - \int_{\mathcal{C}} dx_1 \rho(x_1) \int_{\mathcal{C}} dx_2 \rho(x_2) \tag{B.8}$$

which vanishes since the eigenvalue density is normalized to unity.

In conclusion, we have shown that (B.1) holds and thus the two expressions for the entanglement entropy are equal.

References

[1] J. Erickson, G. Semenoff, and K. Zarembo, "Wilson loops in N=4 supersymmetric Yang-Mills theory," *Nucl.Phys.* **B582** (2000) 155–175, arXiv:hep-th/0003055 [hep-th].

[2] N. Drukker and D. J. Gross, "An Exact prediction of N=4 SUSYM theory for string theory," *J.Math.Phys.* **42** (2001) 2896–2914, arXiv:hep-th/0010274 [hep-th].

[3] V. Pestun, "Localization of gauge theory on a four-sphere and supersymmetric Wilson loops," *Commun.Math.Phys.* **313** (2012) 71–129, arXiv:0712.2824 [hep-th].

[4] A. Lewkowycz and J. Maldacena, "Exact results for the entanglement entropy and the energy radiated by a quark," *JHEP* **1405** (2014) 025, arXiv:1312.5682 [hep-th].

[5] H. Casini, M. Huerta, and R. C. Myers, "Towards a derivation of holographic entanglement entropy," *JHEP* **1105** (2011) 036, arXiv:1102.0440 [hep-th].

[6] J. M. Maldacena, "Wilson loops in large N field theories," *Phys.Rev.Lett.* **80** (1998) 4859–4862, arXiv:hep-th/9803002 [hep-th].

[7] S.-J. Rey and J.-T. Yee, "Macroscopic strings as heavy quarks in large N gauge theory and anti-de Sitter supergravity," *Eur.Phys.J.* **C22** (2001) 379–394, arXiv:hep-th/9803001 [hep-th].

[8] J. Gomis and F. Passerini, "Holographic Wilson Loops," *JHEP* **0608** (2006) 074, arXiv:hep-th/0604007 [hep-th].

[9] J. Gomis and F. Passerini, "Wilson Loops as D3-Branes," *JHEP* **0701** (2007) 097, arXiv:hep-th/0612022 [hep-th].

[10] S. Yamaguchi, "Wilson loops of anti-symmetric representation and D5-branes," *JHEP* **0605** (2006) 037, arXiv:hep-th/0603208 [hep-th].

[11] E. D'Hoker, J. Estes, and M. Gutperle, "Gravity duals of half-BPS Wilson loops," *JHEP* **0706** (2007) 063, arXiv:0705.1004 [hep-th].

[12] O. Lunin, "On gravitational description of Wilson lines," *JHEP* **0606** (2006) 026, arXiv:hep-th/0604133 [hep-th].

[13] E. D'Hoker, J. Estes, and M. Gutperle, "Exact half-BPS Type IIB interface solutions. I. Local solution and supersymmetric Janus," *JHEP* **0706** (2007) 021, arXiv:0705.0022 [hep-th].

[14] E. D'Hoker, J. Estes, and M. Gutperle, "Exact half-BPS Type IIB interface solutions. II. Flux solutions and multi-Janus," *JHEP* **0706** (2007) 022, arXiv:0705.0024 [hep-th].

[15] S. Yamaguchi, "Bubbling geometries for half BPS Wilson lines," *Int.J.Mod.Phys.* **A22** (2007) 1353–1374, arXiv:hep-th/0601089 [hep-th].

[16] S. Ryu and T. Takayanagi, "Holographic derivation of entanglement entropy from AdS/CFT," *Phys.Rev.Lett.* **96** (2006) 181602, arXiv:hep-th/0603001 [hep-th].

[17] S. Ryu and T. Takayanagi, "Aspects of Holographic Entanglement Entropy," *JHEP* **0608** (2006) 045, arXiv:hep-th/0605073 [hep-th].

[18] T. Okuda and D. Trancanelli, "Spectral curves, emergent geometry, and bubbling solutions for Wilson loops," *JHEP* **0809** (2008) 050, arXiv:0806.4191 [hep-th].

[19] J. Gomis, S. Matsuura, T. Okuda, and D. Trancanelli, "Wilson loop correlators at strong coupling: From matrices to bubbling geometries," *JHEP* **0808** (2008) 068, arXiv:0807.3330 [hep-th].

[20] D. Bak, M. Gutperle, and S. Hirano, "A Dilatonic deformation of AdS(5) and its field theory dual," *JHEP* **0305** (2003) 072, arXiv:hep-th/0304129 [hep-th].

[21] R. Benichou and J. Estes, "Geometry of Open Strings Ending on Backreacting D3-Branes," *JHEP* **1203** (2012) 025, arXiv:1112.3035 [hep-th].

[22] A. Lewkowycz and J. Maldacena, "Generalized gravitational entropy," *JHEP* **1308** (2013) 090, arXiv:1304.4926 [hep-th].

[23] K. Jensen and A. O'Bannon, "Holography, Entanglement Entropy, and Conformal Field Theories with Boundaries or Defects," *Phys.Rev.* **D88** no. 10, (2013) 106006, arXiv:1309.4523 [hep-th].

[24] J. Estes, K. Jensen, A. O'Bannon, E. Tsatis, and T. Wrase, "On Holographic Defect Entropy," *JHEP* **1405** (2014) 084, arXiv:1403.6475 [hep-th].

[25] M. Chiodaroli, M. Gutperle, and L.-Y. Hung, "Boundary entropy of supersymmetric Janus solutions," *JHEP* **1009** (2010) 082, arXiv:1005.4433 [hep-th].

[26] M. Chiodaroli, M. Gutperle, and D. Krym, "Half-BPS Solutions locally asymptotic to AdS(3) x S**3 and interface conformal field theories," *JHEP* **1002** (2010) 066, arXiv:0910.0466 [hep-th].

[27] M. Chiodaroli, E. D'Hoker, Y. Guo, and M. Gutperle, "Exact half-BPS string-junction solutions in six-dimensional supergravity," *JHEP* **1112** (2011) 086, arXiv:1107.1722 [hep-th].

[28] T. Azeyanagi, A. Karch, T. Takayanagi, and E. G. Thompson, "Holographic calculation of boundary entropy," *JHEP* **0803** (2008) 054–054, arXiv:0712.1850 [hep-th].

[29] E. D'Hoker, J. Estes, M. Gutperle, and D. Krym, "Exact Half-BPS Flux Solutions in M-theory. I: Local Solutions," *JHEP* **0808** (2008) 028, arXiv:0806.0605 [hep-th].